

# Alma Mater Studiorum Università di Bologna Archivio istituzionale della ricerca

Calvin-Benson cycle regulation is getting complex

This is the final peer-reviewed author's accepted manuscript (postprint) of the following publication:

Published Version: Calvin-Benson cycle regulation is getting complex / Gurrieri L.; Fermani S.; Zaffagnini M.; Sparla F.; Trost P.. - In: TRENDS IN PLANT SCIENCE. - ISSN 1360-1385. - ELETTRONICO. - 26:9(2021), pp. 898-912. [10.1016/j.tplants.2021.03.008]

Availability: This version is available at: https://hdl.handle.net/11585/851372.2 since: 2022-02-02

Published:

DOI: http://doi.org/10.1016/j.tplants.2021.03.008

Terms of use:

Some rights reserved. The terms and conditions for the reuse of this version of the manuscript are specified in the publishing policy. For all terms of use and more information see the publisher's website.

This item was downloaded from IRIS Università di Bologna (https://cris.unibo.it/). When citing, please refer to the published version.

(Article begins on next page)

- 1 HIGHLIGHTS
- 2
- Two enzymes of the Calvin-Benson cycle, GAPDH and PRK, together with the
   regulatory protein CP12, can assemble into an inactive multimeric complex. With the
   recent characterization of the structures of free PRK and GAPDH/CP12/PRK ternary
   complexes, the hierarchical process of aggregation can be described at molecular
   definition.
- 8
- CP12-complexes are conserved in oxygenic phototrophs, but land plants also
   contain an auto-assembling GAPDH isoform, evolutionary derived from CP12. Both
   types of complexes form in the dark and dissociate in light, mainly under the control
   of thioredoxins and pyridine nucleotides.
- 13
- CP12 is a major light/dark regulator of the Calvin-Benson cycle in cyanobacteria and
   contributes to the more sophisticated regulation of the cycle in land plants, where
   dark-complexes may play an additional role in protecting enzymes from proteolysis.
- 17
- 18 TITLE

# 19 CALVIN-BENSON CYCLE REGULATION IS GETTING COMPLEX

20

# 21 AUTHOR NAMES

- 22 Libero Gurrieri<sup>1</sup>, Simona Fermani<sup>2,3</sup>, Mirko Zaffagnini<sup>1</sup>, Francesca Sparla<sup>1</sup>, Paolo Trost<sup>1</sup>
- 23
- <sup>1</sup>Department of Pharmacy and Biotechnology, University of Bologna, Bologna, Italy, I-40126
- 25 <sup>2</sup>Department of Chemistry Giacomo Ciamician, University of Bologna, Bologna, Italy, I-40126
- <sup>3</sup>CIRI Health Sciences & Technologies (HST), University of Bologna, Bologna, Italy, I-40126
- 27
- 28 Corresponding author: <a href="mailto:paolo.trost@unibo.it">paolo.trost@unibo.it</a> (P. Trost);
- 29 <u>https://fabit.unibo.it/en/research/research-groups/research-group-molecular-plant-</u>
- 30 physiology-coordinator-trost; twitter @paotrost
- 31

# 32 **KEYWORDS**

- 33 Redox regulation, protein complexes, photosynthesis, metabolism
- 34

#### 35 ABSTRACT

#### 36

37 Oxygenic phototrophs use the Calvin-Benson cycle to fix CO<sub>2</sub> during photosynthesis. In the 38 dark, glyceraldehyde-3-phosphate dehydrogenase (GAPDH) and phosphoribulokinase 39 (PRK), two enzymes of the Calvin-Benson cycle, form an inactive complex with the 40 regulatory protein CP12, mainly under the control of thioredoxins and pyridine nucleotides. 41 In the light, complex dissociation allows GAPDH and PRK reactivation. GAPDH/CP12/PRK 42 complexes are conserved from cyanobacteria to angiosperms and coexist, in land plant 43 species, with auto-assembling GAPDH complexes that are analogously regulated. The 44 recently described three-dimensional structures of all the elements of this ubiquitous 45 regulatory system, together with novel genome editing techniques, opens a new avenue 46 for understanding the regulatory potential of photosynthetic carbon fixation by in vivo site-47 specific mutagenesis.

#### 48

#### 49 **MAIN TEXT**

50

# 51 The Calvin-Benson cycle is the photosynthetic carbon reduction cycle of oxygenic 52 phototrophs

Photosynthesis is fundamentally a redox process. Fixation of one C atom from CO2 53 54 (oxidation state +4) into a C atom of a sugar (average oxidation state 0) requires four 55 electrons that in oxygenic photosynthetic organisms are provided by the oxidation of two 56 water molecules by the Oxygen Evolving Complex (OEC) of Photosystem II. In essence, 57 oxygenic photosynthesis thus transfers electrons from water to carbon through a light-driven 58 electron transport chain that starts with the OEC and ends up with an oxidoreductase, that 59 is NAD(P)H-dependent glyceraldehyde-3-phosphate dehydrogenase (GAPDH) (Figure 1). 60 GAPDH does not reduce CO<sub>2</sub> directly, but it catalyzes the reaction that gives to the Calvin-Benson cycle its alternative names of photosynthetic carbon reduction cycle or reductive 61 62 carbon fixation pathway [1,2] that underline the redox nature of this metabolism.

63

By mounting a CO<sub>2</sub> molecule on a sugar, Rubisco generates the organic acid that GAPDH will reduce to sugar again, thereby creating the conditions to reconstitute the substrate of Rubisco and set aside the fixed carbon in the form of sugar-phosphates (**Figure 1**). The Rubisco reaction is exergonic but the whole cycle requires three ATP per CO<sub>2</sub>: two ATPs are used by phosphoglycerate kinase (PGK) to activate the products of Rubisco prior to reduction by GAPDH, and one ATP is used for the regeneration of the substrate of Rubisco by phosphoribulokinase (PRK) (Figure 1). The two kinases together with three
dephosphorylation steps allow the cycle to proceed spontaneously in one-way direction if
sufficient ATP is made available by light reactions of photosynthesis.

73

74 Four consecutive reactions of the cycle depend on external inputs: phosphoribulokinase 75 (ATP), Rubisco (CO<sub>2</sub>), phosphoglycerate kinase (ATP) and GAPDH (NADPH). The first and last 76 enzyme of this metabolic sequence are redox-regulated and can assemble into an inactive 77 complex with a third partner protein known as CP12 (Figure 1). Reversible complex 78 formation and modulation of GAPDH and PRK activities are mainly controlled by the 79 thioredoxins redox state, and by tris-phosphorylated (NADP<sup>+</sup> and NADPH) versus bis-80 phosphorylated pyridine nucleotides (NAD<sup>+</sup> and NADH). Both parameters are perturbed by 81 light/dark or stress conditions and provide a link between Calvin-Benson cycle regulation 82 and environmental cues [3-6].

83

From cyanobacteria to land plants, all oxygenic photosynthetic organisms use the Calvin-Benson cycle to fix CO<sub>2</sub>, and with a few exceptions, all contain CP12 (**Box 1**). Non-oxygenic phototrophic bacteria may contain a Calvin-Benson cycle based on deeply divergent enzymes in respect to cyanobacteria, but they do not have CP12 [7-10]. In this review, we provide a view of the regulation of the Calvin-Benson cycle, based on both functional studies and the recently solved atomic structures of all components and complexes of the CP12-regulatory system in different oxygenic phototrophs.

91

## 92 Phosphoribulokinase, the kinase that prepares the substrate for Rubisco

93 PRK belongs to the nucleoside/nucleotide kinase superfamily [11] and exists in three types: 94 plant-type, found in most cyanobacteria, plants (Plantae) and photosynthetic protists; 95 archeal-type and bacterial-type, the latter in proteobacteria and in oceanic a-96 cyanobacteria that contain bacterial-type Rubisco form 1A and no canonical CP12 genes 97 [12-14]. Plant and archeal-types are dimeric and share a similar structure [14-17] while 98 bacterial PRK is octameric with monomers showing limited structural similarity to 99 plant/archeal types [18]. Among the three types, only plant-type PRK contain regulatory 100 cysteines whose redox state is controlled by thioredoxins (TRXs) and coexists with CP12, 101 which provides a further level of regulation (Box 1).

102

103 The structure of plant-type PRKs became available only in 2019 [14,16,17,19]. The core 104 structure of the dimer is an extended mixed  $\beta$ -sheet formed by nine  $\beta$ -strands per subunit, surrounded by additional secondary structures (**Figure 2**). The N-terminal regions, at the two ends of the  $\beta$ -sheet, show the characteristic nucleoside/nucleotide kinase superfamily fold and harbor the active sites [14]. Dimerization between C-terminal regions involves a single  $\beta$ -strand for each monomer and a dimer interface of about 550 Å<sup>2</sup>, smaller than in both archeal and bacterial PRKs (~ 1,550 Å<sup>2</sup>, [15,18]) and indicative of structural flexibility (**Figure 3**) [16]. C-terminal regions underwent extensive rearrangements along evolution of the three PRK types and are structurally more variable than N-terminal regions [14-16,18].

- The active site includes a positive groove that provides complementary charges for the phosphate groups of ribulose-5-phosphate (Ru5P) and ATP (**Figure 2**) [14,16,17]. The characteristic P-loop of nucleotide-binding proteins contributes to the bonding network that places the ATP γ-phosphate near the carbon-1 of Ru5P. Between them Asp58 and His106 act as a catalytic base that activates the carbon-1 of Ru5P thereby favoring the attack of the γ-phosphate of ATP (**Figure 2**). No phospho-enzyme intermediate is necessary during catalysis [17].
- 120

Binding assays pointed out an obligate sequence for substrates entry. ATP is bound first and causes a conformational change that permits Ru5P to fit in its pocket [17]. A structural study on a kinase of the same superfamily (uridine-cytidine kinase; [20]) suggests that the movement of a helical hairpin usually referred as the lid determines the order of substrate binding [14]. When PRK is bound to CP12 in the ternary complex, the lid is fixed in open conformation by CP12 itself (**Figure 2E**).

127

Together with CP12, PRK is part of the minimal redox toolkit that controls the carbon flux in 128 129 day/night cycles in cyanobacteria [21]. PRK regulation, based on disulfides that can form 130 in either PRK or CP12, is conserved in cyanobacteria and along the green lineage [10] (Box 131 1). Regulatory cysteines of the N-terminal region (Cys15/Cys54 in arabidopsis (Arabidopsis 132 thaliana) and Cys16/Cys55 in Chlamydomonas reinhardtii [16]) are responsible for the 133 oxidative inactivation of PRK itself [22] (Figure 2D). Cys15 (arabidopsis numbering in the 134 following) is contained in the P-loop which flips to allow the formation of the disulfide with 135 Cys54 [14,17,19]. The reactivity of Cys15 is ensured by a conserved molecular environment 136 within the P-loop [16,17]. Plant-type PRKs may form a second disulfide in the C-terminal 137 region [14,16,23] (Figure 2A) which is found when the enzyme is in complex with GAPDH and 138 CP12 [17,19]. The C-terminal disulfide does not affect the activity but appears necessary for 139 GAPDH/CP12/PRK assembly in Chlamydomonas reinhardtii [23].

140

141 TRX f is the most efficient reductant of PRK N-terminal disulfide [16,22,24]. The interaction 142 between TRX f and PRK was proposed to be mediated by complementary charges around 143 Cys54 in PRK and active site cysteines in TRX f [16,25]. In an alternative model, a 144 conformational swing of the flexible clamp loop of PRK would be required to expose Cys54 145 to the TRX attack [17]. The clamp loop is found in algae and plants (that contain TRX f), but 146 not in cyanobacteria that do not contain TRX f [10,16,17,26]. Notwithstanding the still debated role of the clamp loop, the presence of flexible elements in plant-type PRKs (dimer 147 148 interface, lid, clamp loop) confers conformational adaptability to more rigid partners like 149 TRXs and GAPDH.

150

# Glyceraldehyde-3-phosphate dehydrogenase, the enzyme of the photosynthetic carbonreduction

153

Land plants genomes typically contain four different types of GAPDH genes (GAPA, GAPB, GAPC, GAPCp) whose protein products form four tetrameric isoforms (A<sub>4</sub> and A<sub>2</sub>B<sub>2</sub> in chloroplasts; C<sub>4</sub> in the cytosol; Cp<sub>4</sub> in heterotrophic plastids). Green algae and cyanobacteria contain only A<sub>4</sub>- and C<sub>4</sub>-GAPDH isoforms (**Box 1**).

158

159 The 3D structure is known and well conserved in all GAPDH isoforms (Figure 3). Each subunit 160 contains a catalytic domain that binds the substrate, and a cofactor-binding domain that 161 binds, in the same position, either NAD(H) or NADP(H). An S-loop belonging to the adjacent 162 subunit contributes to cofactor stabilization and recognition [27,28]. Specificity toward 163 pyridine nucleotides varies from glycolytic GAPDH isoforms C<sub>4</sub> and Cp<sub>4</sub>, that are NAD(H)-164 specific, to  $A_4$  and  $A_2B_2$ -GAPDH of the Calvin-Benson cycle that can use both NADP(H) and 165 NAD(H) (**Box 1**). Bispecific GAPDHs (A<sub>4</sub>, A<sub>2</sub>B<sub>2</sub>) are typically regulated by interaction with CP12 166 and PRK, but A<sub>2</sub>B<sub>2</sub>-GAPDH is also specifically regulated in a CP12-independent manner [29].

167

In NADPH, the ribose closest to the adenine is 2'-phosphorylated compared with NADH that carries a hydroxyl group in the same position. In GAPDH isoforms that bind NAD(H), the 2'hydroxyl of NAD(H) makes a hydrogen bond with Asp32, whose fixed position prevents NADP(H) from binding [28]. Bispecific GAPDHs (A4 and A2B2) can substitute NAD(H) with NADP(H) by letting Asp32 to rotate away from the extra-phosphate. Residues Arg77, Thr33 and Ser188 (*Spinacia oleracea* numbering [30]) interact with the NADP(H) 2'-phosphate (**Figure 3**). NADP(H) recognition results in faster NADP(H) vs. NAD(H)-dependent catalysis, in

175 spite of the identical redox properties of the two coenzymes. Replacement of specific 176 NADP(H)-interacting residues with non-interacting ones results in GAPDH mutants with 177 decreased NADP(H)-dependent activity, but similar NADH-dependent activity [30,31]. 178 Understanding coenzyme recognition is important for understanding GAPDH regulation 179 because it specifically affects the NADP(H)-dependent activity, leaving the NAD(H)-180 dependent one unaffected [29].

181

182 The catalytic domain contains two anion recognition sites, named Pi and Ps, which harbour 183 the phosphate groups of BPGA (Figure 3). In the Ps site, the thiolate of Cys149, activated by 184 His176, makes a covalent bond with the substrate prior to its reduction. As detailed below, 185 GAPDH may participate in different types of complexes (e.g. A<sub>4</sub>-GAPDH/CP12/PRK, A<sub>8</sub>B<sub>8</sub>-186 GAPDH) without significantly changing the overall structure of the tetramer which appears 187 remarkably rigid (Figures 3,4). Flexible partners need to adapt to GAPDH, not viceversa, a 188 concept that is probably valid also for the manifold interactions that glycolytic C<sub>4</sub>-GAPDH 189 displays in its moonlighting functions [32,33].

- 190
- 191

#### CP12, the PRK/GAPDH regulatory protein

192

193 CP12 is an intrinsically disordered protein of about 80 amino acids [8,9,34-36] that adopts a 194 defined tridimensional structure after binding to its partners GAPDH and PRK. Canonical 195 CP12 is characterized by four conserved cysteines able to form two disulfide bridges and 196 the consensus sequence AWD\_VEEL. The N-terminal region of CP12 contains one of the two 197 cysteine pairs followed by the consensus sequence which is involved in PRK binding. The C-198 terminal region contains the second cysteine pair and binds GAPDH. Genes coding for 199 canonical CP12 are present in almost all genomes of organisms that fix CO<sub>2</sub> via the Calvin-200 Benson cycle, in particular cyanobacteria, green algae and land plants [9,8] (Box 1). 201 Notable exceptions include oceanic a-cyanobacteria which contain only CP12 genes with 202 neither the N-terminal disulfide nor the consensus sequence [13], and prasinophycean 203 green algae like Ostreococcus tauri which contain no CP12 genes at all [37]. On the other 204 hand, Ostreococcus species are the only green algae (Chlorophyta) known to contain 205 redox-regulated B subunits of GAPDH, which are typical of Streptophyta (land plants and 206 charophycean algal ancestors) [38].

207

208 The disulfide bridges of CP12 are formed in the presence of oxidized TRX [24] or other 209 oxidants (GSSG, H<sub>2</sub>O<sub>2</sub>)[39], and the C-terminal disulfide requires less oxidizing power than

- the N-terminal one ( $E_{m,7.9}$  -352 and -326 mV, respectively, in arabidopsis CP12-2)[40]. The Nterminal region of CP12, from either arabidopsis or Anabaena, was recently exploited to develop FRET-based sensors detecting the thioredoxin redox state *in vivo* [5].
- 213

214 Although oxidized CP12 remains essentially disordered, a local structural motif in the C-215 terminal domain is stabilized by its disulfide bridge, allowing the interaction with GAPDH and 216 thus the initiation of the ternary complex assembly [41,42]. Based on this property, CP12 has 217 been defined as a conditionally rather than intrinsically disorderd protein [42]. The oxidized 218 N-terminal domain folds into a stable two-helix bundle only after CP12 has bound to GAPDH 219 [19,43] or to other protein domains like in cyanobacterial fusion proteins with cystathionine 220 β-synthase domains (CP12-CBS; **Box 1**)[13,44]. In any case, the N- and C-terminal domains 221 of CP12 are connected by a flexible linker that remains flexible even when the rest of CP12 222 is fully folded [17,19] (Figure 2).

223

# 224 GAPDH/CP12, the intermediate complex that recruits PRK

225

The GAPDH/CP12 association is the first obligatory step of the hierarchical assembly of the ternary complex with PRK [40,45] (**Figure 1**). Two prerequisites allow the interaction to occur: GAPDH has to be loaded with NAD(H), rather than NADP(H), and CP12 has to bear the Cterminal disulfide. The structure of the GAPDH/CP12 complex has been solved from arabidopsis [41] and two different cyanobacteria [19,46].

231

232 The binding of disordered CP12 to rigid GAPDH implies an entropic penalty (5 kcal mol<sup>-1</sup>) as 233 CP12 becomes ordered, that has to be counteracted by enthalpy (energy released by 234 novel interactions, -15 kcal mol<sup>-1</sup>; 40]. The mechanism of formation of the GAPDH/CP12 235 binary complex of arabidopsis was proposed to involve a conformational selection step 236 (GAPDH binds a defined local conformation of CP12) followed by an induced folding step, 237 in which CP12 slips into the active site of GAPDH where it is stabilized by an extensive network 238 of hydrogen bonds [41]. As a result, P-sites of GAPDH are fully occupied by CP12, and Glu72 239 of CP12 occupies the binding site for the 2'-phosphate group of NADP(H) [41,46](Figure 3). 240 For this structural reason, the GAPDH/CP12 complex is stable in the presence of NAD(H) 241 while NADP(H) can disrupt the complex and counteract the inhibition of the NADP(H)-242 dependent activity of GAPDH [45,47,48]. In the binary complex, the NAD(H)-dependent 243 activity is instead inhibited because the binary complex is stable and only two active sites 244 out of four can perform the catalysis [19] (Figure 3).

245

## 246 GAPDH/CP12/PRK, the complex of temporarily inactivated enzymes

247

The ternary complex consist of two GAPDH tetramers and two PRK dimers linked by four oxidized CP12 and results from the capability of GAPDH/CP12 binary complexes to bind PRK dimers [35,39,45,49] (**Figure 3**). Similar atomic structures of GAPDH/CP12/PRK complexes were recently obtained by cryo-EM from the cyanobacterium *Thermosynechococcus elongatus* [19] and X-ray crystallography from *Arabidopsis thaliana* [17]. The ternary complex shows a spindle-shape with a hole in the middle, GAPDH tetramers at the two tips and two CP12/PRK/CP12 elements connecting them (**Figure 1 and 3**).

255

256 Once formed the GAPDH/CP12 complex, the oxidized N-terminal domain of CP12 folds into 257 a two-helical bundle [19] that may plug into the PRK active site [17] (**Figure 2**). Positive 258 residues of PRK, mainly belonging to the P-loop and lid, and normally involved in phosphates 259 binding, interact with the negative consensus sequence of CP12 (AWD\_VEEL)[14,16,17,19]. 260 Accommodation of CP12-helical bundle in the catalytic groove of PRK fixes the lid in open 261 conformation [19].

262

263 Whether the redox state of PRK disulfides is relevant for complex formation is not yet clear. 264 Oxidation of C-terminal cysteines may fix PRK in a favorable conformation for complex 265 assembly [23] and indeed, the C-terminal cysteines of ternary complex PRK are usually, but 266 not always, engaged in a disulfide [17,19]. Conversely, the N-terminal disulfide is probably 267 dispensable as even in the complex, the P-loop of PRK can flip and promote the formation 268 of the disulfide without clashing with CP12 [17]. Thanks to their flexibility [16], complexed 269 PRKs can assume a twisted conformation compared to free PRKs [17,19] and CP12/PRK 270 binding is slightly different in different species [17]. In general, the young components of the 271 systems (in evolutionary terms, PRK and CP12, [50]) seem to adjust their conformations to 272 the firm structure of old GAPDH tetramers, and not viceversa.

273

Ternary complex structures clearly show that 100% of PRK- and 50% of GAPDH-active sites are blocked by CP12, and that CP12 interferes with coenzyme binding in the remaining GAPDH subunits (**Figure 3**). Since PRK in the complex can exist in different redox states [51,52], CP12 provides a way to inhibit PRK activity independently from PRK redox regulation. Moreover, CP12 is the only way to regulate A<sub>4</sub>-GAPDH. Experimentally measured, both PRK and GAPDH activities of the complex are strongly inhibited but total inhibition is never

280 observed because the substrates of the reactions (ATP, BPGA, NADPH) may all contribute 281 to complex dissociation by competing with CP12-binding sites [43,47,48,52] (Figure 4). In vitro 282 at least, the higher plant complex is dissociated in the minutes time scale  $(t_{1/2} 0.3 - 0.6 \text{ min})$  [24] 283 upon reduction of the N-terminal disulfide of CP12 by TRX f [17,24]. Interestingly, PRK 284 reactivation by TRXs is faster when PRK is part of the ternary complex than free oxidized form, 285 suggesting that CP12 represent a quicker way to control PRK activity [24]. Overall CP12 acts 286 as an entropy-driven redox switch that triggers complex dissociation when it is reduced and 287 the resulting increase in entropy is the driving force for prompt reactivation of enzymes 288 activities [40].

289

290 Besides the canonical binary (GAPDH/CP122) and ternary complexes here described 291 (GAPDH<sub>2</sub>/CP12<sub>4</sub>/PRK<sub>2</sub>), further possibilities may exist. For instance, GAPDH-CP12<sub>4</sub> complexes 292 were obtained in vitro with cyanobacteria proteins at high CP12:GAPDH ratios [19, 46] and 293 reconstituted GAPDH/CP12/PRK complexes of Chlamydomonas reinhardtii were found to 294 bind aldolase in vitro with strong affinity ( $K_D$  55 nM) [53]. Whether these complexes do exist 295 in vivo in chlamydomonas or other organisms is currently unknown. In higher plants at least, 296 the CP12-complexes that could be extracted from tobacco plants did not contain any 297 other protein than GAPDH (A and B subunits) and PRK [54].

298

# 299 The A<sub>2</sub>B<sub>2</sub>-GAPDH isoform of land plants has acquired from CP12 its regulatory properties

300

301 In land plants and charophycean algal ancestors (Streptophytes) CP12 coexists with A<sub>2</sub>B<sub>2</sub>-302 GAPDH, which is a regulated version of A<sub>4</sub>-GAPDH [37, 55-57] (Box 1). All regulatory 303 properties of A<sub>2</sub>B<sub>2</sub>-GAPDH depend on the C-terminal extension (CTE) of B-subunits that is 304 homologous to the C-terminal domain of CP12 [56,58]. Similar to  $A_4$ -GAPDH, fully active  $A_2B_2$ -305 GAPDH shows a marked kinetic preference for NADPH over NADH based on both higher 306  $V_{max}$  (1.5-fold) and 5-fold lower  $K_m$  [30,31]. The kinetic preference is based on proper 307 coenzyme recognition and abolished in oxidized A<sub>2</sub>B<sub>2</sub>-GAPDH, that carries a disulfide bridge 308 in the CTE and uses NADPH and NADH with similar and low efficiency [58].

309

When the CTE, which is negatively charged, is oxidized, it is attracted by the positive cleft between A and B subunits, the same cleft occupied by CP12 in GAPDH/CP12 complexes (**Figure 3**). However, the position of the CTE is less deep within the cleft and its C-terminus does not reach the P-sites like CP12 [17,19,46,59]. Nevertheless the NADP(H)-dependent activity is inhibited because none of the residues involved in NADP(H) recognition (Ser188; 315 Thr33; Arg77) are correctly in place [59]. Arg77 is displaced from its normal position, possibly 316 because attracted by negative charges of the CTE. Ser188 and Thr33 do not interact with 317 NADP<sup>+</sup> either (Figure 3). As a result, the 2'- phosphate of NADP(H) is either completely free 318 (in subunits B) or (in subunits A) loosely interacting with the last residue of the CTE (Glu362), 319 itself engaged in a salt bridge that anchors the CTE to the cleft [59]. Consistent with the 320 concept that the kinetic preference for NADP(H) depends on the capability to recognize 321 NADP(H) from NAD(H), the NADPH-activity is down-regulated to the level of the constitutive 322 NADH-dependent one [31,58]. Mutants analyses were consistent with this model: by 323 introducing single mutations it was possible to convert a redox-sensitive GAPDH (with B-324 subunits) into a redox-insensitive GAPDH (A4-like), or an A4-GAPDH (behaving like 325 reduced/activated A<sub>2</sub>B<sub>2</sub>-GAPDH) into an oxidized/inhibited A<sub>2</sub>B<sub>2</sub>-like GAPDH [30,31,59].

326

327 Understanding the regulation of A<sub>2</sub>B<sub>2</sub>-GAPDH is complicated by the fact that when bound 328 NADP(H) is substituted by NAD(H), the oxidation of the CTE causes the aggregation of the 329 tetramers in inhibited multimeric complexes (mainly A<sub>8</sub>B<sub>8</sub>, but also A<sub>4</sub>B<sub>4</sub> and others, 330 [55,58,60,61]). Inhibited complexes of A<sub>2</sub>B<sub>2</sub> are the only members of the GAPDH/PRK 331 regulatory system whose atomic structure has not been yet described.

332

# Relevance and *in vivo* evidence of CP12-dependent and independent regulation of the Calvin-Benson cycle

335

336 Both PRK, CP12 and A<sub>2</sub>B<sub>2</sub>-GAPDH contain cysteines able to form disulfide bridges with 337 negative effects on enzyme activities and positive effects on complex formation (Figure 4). 338 In vitro, such disulfides are efficiently reduced by TRXs f and m [24] whose redox states, in 339 vivo, tend to be reduced in the light [5,62]. Under same conditions, PRK and  $A_2B_2$ -GAPDH 340 are also found reduced, enzymatically active and free from complexes in different higher 341 plant species [52,54,60,62-66]. The reduction/activation/dissociation state of both GAPDH 342 and PRK correlate with light intensity in the minute-time scale and is blocked by inhibitors of 343 the photosynthetic electron transport chain required to reduce TRXs [52,62]. Besides TRXs, 344 NTRC does also contribute to reduction/activation of the system, possibly by direct 345 interaction with PRK [63,66].

346

In the dark, PRK and GAPDH (and TRXs f/m) are conversely detected in oxidized form [6367]. Electrons derived from disulfide bridge formation are shuttled to 2-cys peroxiredoxins
(2CP) by atypical TRXs ACHT and TRXL2, with hydrogen peroxide acting as final electron

acceptor [65-68] (Figure 4). In vitro, hydrogen peroxide may directly induce disulfide bridges
 formation in CP12, and A<sub>4</sub>-GAPDH, whose catalytic cysteine is highly sensitive to H<sub>2</sub>O<sub>2</sub> oxidation to sulfinic acid, is fully protected when assembled in ternary complex with CP12
 [39]. Whether this protective mechanism is operative also *in vivo* is currently unknown.

354

355 Activities of both PRK and GAPDH rapidly drop in the dark in wild type arabidopsis plants 356 but much more slowly in 2CP-knock out mutants [65,66]. Dark-inactivation takes few minutes 357 and correlate with the sequestration of GAPDH and PRK in CP12-complexes [52,61] and 358 A<sub>8</sub>B<sub>8</sub>-GAPDH [60,62], although not in all species and with all techniques dark-complexes are 359 easily detected [61,69]. In most species, PRK is found fully sequestered in dark-complexes 360 but some GAPDH remains as free tetramers (A<sub>2</sub>B<sub>2</sub>; A<sub>4</sub>) [52,61]. Recent quantifications of 361 Calvin-Benson cycle enzymes in Chlamydomonas reinhardtii consistently showed that A-362 subunits of GAPDH exceed PRK subunits by a factor of 4 [70]. Since the GAPDH/PRK subunit 363 ratio of the ternary complex is invariably 2 [17,19,52] (Figure 3) we argue that, in 364 Chlamydomonas at least, there's no enough PRK to sequestrate all GAPDH in dark-365 complexes.

366

The existence of ternary complexes implies that also CP12 must be oxidized in the dark *in* vivo, in agreement with *in vitro* redox potential determinations [24]. It is also known from *in* vitro studies that GAPDH/CP12/PRK and A<sub>8</sub>B<sub>8</sub>-GAPDH are stabilized by low NADP(H)/NAD(H) ratios that seem to be established in darkened chloroplasts [71,4] and in cyanobacteria [48,72] thereby favoring dark-complexes stability (**Figure 4**).

372

Altogether, plenty of *in vivo* evidence support the notion that oxygen phototrophs temporarily store PRK and GAPDH in inactive complexes of known atomic structure under low photosynthetic conditions or in the dark, and dissociate such complexes to release the active enzymes during illumination. The relative importance of thioredoxin redox state, NAD(H)/NADP(H) ratios or activating metabolites like BPGA and ATP in the equilibrium between ternary complex and free enzymes *in vivo* remains to be understood.

379

Further studies demonstrated, particularly in cyanobacteria, that the CP12-complex is important for regulating the Calvin-Benson cycle under diel light/dark cycles. A mutant strain of Synechococcus PCC7942 lacking a canonical CP12, grew normally in continuous light but slower than wild type cells in 12h/12h light/dark cycle, indicating that darkinactivation of GAPDH and PRK is not dispensable [48]. Marine a-cyanobacteria like

385 Prochlorococcus which do not contain a canonical CP12 gene in their genome [73] (Box 1) can be infected by cyanophages (bacteriophages that infect cyanobacteria) that do 386 387 contain a CP12 gene in their genome of only 24 genes [72]. Optimal reproduction for these 388 parasites requires ATP and NADPH produced by light reactions of photosynthesis. The 389 expression of phage CP12 in infected cells is induced in the light and the resulting inhibition 390 of the Calvin-Benson cycle from PRK to GAPDH diverts photosynthetically produced ATP 391 and NADPH from carbon fixation to phage replication [73] (Figure 1). The concept that CP12 392 is a master regulator of the Calvin-Benson cycle in cyanobacteria in light/dark conditions 393 was recently exploited in a successful biotechnological strategy aimed in rewiring carbon 394 metabolism in glucose-fed Synechococcus elongatus PCC7942 cells. Deletion of CP12 395 combined with overexpression of PRK, allowed the PRK-to-GAPDH portion of the Calvin-396 Benson cycle to function in the dark in these cells [74], further confirming the role of CP12 in 397 regulating the Calvin-Benson cycle according to light availability. Moreover, many 398 cyanobacterial species contain CP12-CBS proteins in which CP12 is fused to two 399 cystathionine  $\beta$ -synthase domains (**Box 1**). CP12-CBS do not bind GAPDH but can bind and 400 inhibit PRK in an AMP-dependent manner [44].

401

402 In higher plants, the physiological role of CP12 is also complex and not yet fully understood. 403 Arabidopsis thaliana contains three CP12 paralogues with tissue-specific expression 404 [29,9,75,76]. CP12-1 and CP12-2 are closely related and represent a single CP12 form found 405 throughout the higher plants, while CP12-3 represents a divergent CP12 form not universally 406 present in higher plants [8]. In arabidopsis, CP12-1 and CP12-2 are highly expressed in leaves 407 but no phenotypic alterations were observed in single CP12 mutants. On the contrary, 408 transgenic lines with strongly reduced levels of both CP12-1 and CP12-2 were negatively 409 affected in photosynthetic capacity and biomass yield [77]. Intriguingly, the amount of PRK, 410 but not its transcript level, was dramatically reduced in CP12-double mutants, suggesting 411 that the stability of PRK might be under control of CP12 with functional consequence on 412 photosynthetic capacity and growth. While opening a new perspective on a possible role 413 of CP12-complexes in preserving PRK from degradation in the night, these results prevent 414 an easy demonstration of CP12 function in higher plants based on classical reverse genetic 415 approaches.

416

# 417 Concluding remarks and Future perspectives

418

419 GAPDH and PRK, two essential enzymes of the Calvin-Benson cycle are stored as inactive 420 complexes in the dark in most oxygenic phototrophs. Complex assembly depends on the 421 regulatory protein CP12 and, in land plants, also on the CP12-derived C-terminal extension 422 of GAPDH B-subunits. An overarching control on the regulatory system is mediated by the 423 TRXs redox state, pyridine nucleotides and metabolites (ATP and BPGA), allowing 424 inactivated complexes to release active enzymes and viceversa, depending on light 425 conditions and photosynthetic activity. Structure/function relationships in GAPDH and PRK 426 regulation through complex formation are beginning to be understood.

427

428 Reverse genetics, the default approach for studying gene function, is of little use for studying 429 regulatory mechanisms based on post-translational modifications and protein-protein 430 interactions like the CP12-(in) dependent regulation of GAPDH and PRK of the Calvin-Benson cycle. To address these questions, specific amino acids mutations are more informative than 431 432 gene knockouts. This approach requires detailed knowledge of protein structures/function 433 relationships and sophisticated genome editing techniques [78], but we believe that 434 protein-based in vivo studies will soon integrate traditional genomic approaches in plant 435 physiology.

436

#### 437 **REFERENCES**

- 438
- Sharkey, T.D. (2019) Discovery of the canonical Calvin-Benson cycle. Photosynth.
   Res. 140, 235-252
- 441
  2. Bar-Even, A. et al. (2012) A survey of carbon fixation pathways through a
  442 quantitative lens. J. Exp. Bot. 63(6), 2325-42.
- 3. Zaffagnini, M. *et al.* (2019) Redox Homeostasis in Photosynthetic Organisms: Novel
  and Established Thiol-Based Molecular Mechanisms. Antioxid. Redox Signal. 31(3),
  155-210.
- 446
  4. Hashida, S.N. *et al.* (2019) Inter-Organelle NAD Metabolism Underpinning Light
  447
  447 Responsive NADP Dynamics in Plants. Front. Plant Sci. DOI:10.3389/fpls.2019.00960
  448 (<u>https://www.frontiersin.org/journals/plant-science</u>)
- Sugiura, K. *et al.* (2019) The thioredoxin (Trx) redox state sensor protein can visualize
  Trx activities in the light/dark response in chloroplasts. J. Biol. Chem. 294(32), 1209112098.

- 452 6. Li, B.B. *et al.* (2018) NAD Kinases: Metabolic Targets Controlling Redox Co-enzymes
  453 and Reducing Power Partitioning in Plant Stress and Development. Front. Plant Sci.
  454 23, 9:37 (<u>https://www.frontiersin.org/journals/plant-science</u>)
- 455 7. Martin, W. and Schnarrenberger, C. (1997) The evolution of the Calvin cycle from
  456 prokaryotic to eukaryotic chromosomes: a case study of functional redundancy in
  457 ancient pathways through endosymbiosis. Curr. Genet. 32(1), 1-18.
- Groben, R. et al. (2010) Comparative sequence analysis of CP12, a small protein
   involved in the formation of a Calvin cycle complex in photosynthetic organisms.
   Photosynth. Res. 103, 183-194
- 461
  9. Marri, L. *et al.* (2010) In vitro characterization of Arabidopsis CP12 isoforms reveals
  462 common biochemical and molecular properties. J. Plant Physiol. 167, 939-950
- 463 10. Balsera, M. et al. (2014) Evolutionary development of redox regulation in
  464 chloroplasts. Antioxid. Redox. Signal. 21, 1327-1355
- 465 11. Leipe, D.D. et al. (2003) Evolution and classification of P-loop kinases and related
  466 proteins. J. Mol. Biol. 333, 781-815
- 467 12. Tabita F.R. (1999) Microbial ribulose 1,5-bisphosphate carboxylase/oxygenase: a
  468 different perspective. Photosynth. Res. 60, 1–28.
- 469 13. Stanley, D.N. *et al.* (2013) Comparative analysis of 126 cyanobacterial genomes
  470 reveals evidence of functional diversity among homologs of the redox-regulated
  471 CP12 protein. Plant Physiol. 161, 824-835.
- 473 14. Wilson, R.H. et al. (2019) Crystal structure of phosphoribulokinase from

472

- 474 Synechococcus sp. strain PCC 6301. Acta Crystallogr. F Struct. Biol. Commun. 75,
  475 278-289
- 476 15. Kono, T. et al. (2017) A RuBisCO-mediated carbon metabolic pathway in
  477 methanogenic archaea. Nat Commun. 8, 14007. DOI:10.1038/ncomms14007
  478 (https://www.nature.com/ncomms)
- 479 16. Gurrieri, L. et al. (2019) Arabidopsis and Chlamydomonas phosphoribulokinase
  480 crystal structures complete the redox structural proteome of the Calvin-Benson
  481 cycle. Proc. Natl. Acad. Sci. U.S.A. 116, 8048-8053
- 482 17. Yu, A. et al. (2020) Photosynthetic Phosphoribulokinase Structures: Enzymatic
  483 Mechanisms and the Redox Regulation of the Calvin-Benson-Bassham Cycle. Plant
  484 Cell. 32, 1556-1573

- 485 18. Harrison, D.H. *et al.* (1998) The crystal structure of phosphoribulokinase from
  486 Rhodobacter sphaeroides reveals a fold similar to that of adenylate kinase.
  487 Biochemistry. 37, 5074-5085
- 488 19. McFarlane, C.R. et al. (2019) Structural basis of light-induced redox regulation in the
  489 Calvin-Benson cycle in cyanobacteria. Proc. Natl. Acad. Sci. U. S. A. 116, 20984490 20990
- 491 20. Tomoike, F. et al. (2017) Indispensable residue for uridine binding in the uridine492 cytidine kinase family. Biochem. Biophys. Rep. 11, 93-98
- 493 21. Gütle, D. et al. (2017) Dithiol disulphide exchange in redox regulation of chloroplast
  494 enzymes in response to evolutionary and structural constraints. Plant. Sci. 255, 1-11
- 495 22. Brandes, H.K. *et al.* (1996) Efficient expression of the gene for spinach
  496 phosphoribulokinase in *Pichia pastoris* and utilization of the recombinant enzyme to
  497 explore the role of regulatory cysteinyl residues by site-directed mutagenesis. J. Biol.
  498 Chem. 271, 6490-6496.
- 499 23. Thieulin-Pardo, G. *et al.* (2015) Phosphoribulokinase from Chlamydomonas
  500 reinhardtii: a Benson-Calvin cycle enzyme enslaved to its cysteine residues. Mol.
  501 Biosyst. 11, 1134-1145
- 502 24. Marri, L. *et al.* (2009) Prompt and easy activation by specific thioredoxins of calvin
  503 cycle enzymes of Arabidopsis thaliana associated in the GAPDH/CP12/PRK
  504 supramolecular complex. Mol. Plant. 2, 259-269
- 505 25. Lemaire, S.D. et al. (2018) Crystal Structure of Chloroplastic Thioredoxin f2 from
  506 Chlamydomonas reinhardtii Reveals Distinct Surface Properties. Antioxidants (Basel).
  507 7, 171.
- 508 26. Kobayashi, D. *et al.* (2003) Molecular characterization and redox regulation of
  509 phosphoribulokinase from the cyanobacterium Synechococcus sp. PCC 7942. Plant
  510 Cell Physiol. 44, 269-276
- 511 27. Fermani, S. *et al.* (2001) Crystal structure of the non-regulatory A<sub>4</sub>isoform of spinach
  512 chloroplast glyceraldehyde-3-phosphate dehydrogenase complexed with NADP. J.
  513 Mol. Biol. 314, 527-542
- 514 28. Falini, G. et al. (2003) Dual coenzyme specificity of photosynthetic glyceraldehyde-
- 5153-phosphate dehydrogenase interpreted by the crystal structure of A4 isoform516complexed with NAD. Biochemistry. 42, 4631-4639
- 517 29. Trost, P. *et al.* (2006) Thioredoxin-dependent regulation of photosynthetic
- 518 glyceraldehyde-3-phosphate dehydrogenase: autonomous vs. CP12-dependent 519 mechanisms. Photosynth. Res. 89, 263-275.

- 30. Sparla, F. *et al.* (2004) Coenzyme site-directed mutants of photosynthetic A4GAPDH show selectively reduced NADPH-dependent catalysis, similar to regulatory
  AB-GAPDH inhibited by oxidized thioredoxin. J. Mol. Biol. 340, 1025-1037.
- 523 31. Sparla, F. et al. (2005) Regulation of photosynthetic GAPDH dissected by mutants.
  524 Plant Physiol. 138, 2210-2219
- 52532. Zaffagnini, M. et al. (2013) Plant cytoplasmic GAPDH: redox post-translational526modifications and moonlighting properties. Front. Plant Sci. DOI:
- 527 10.3389/fpls.2013.00450 (https://www.frontiersin.org/journals/plant-science)
- 528 33. Kim, S.C. *et al.* (2020) Nuclear moonlighting of cytosolic glyceraldehyde-3529 phosphate dehydrogenase regulates Arabidopsis response to heat stress. Nat.
  530 Commun. 11, 3439. DOI:10.1038/s41467-020-17311-4
- 531 (https://www.nature.com/ncomms)
- 53234. Wedel, N. et al. (1997) CP12 provides a new mode of light regulation of Calvin533cycle activity in higher plants. Proc. Natl. Acad. Sci. U.S.A. 94, 10479-10484
- 53435. Graciet, E. et al. (2003) The small protein CP12: a protein linker for supramolecular535complex assembly. Biochemistry. 42, 8163-8170.
- 536 36. Launay, H. et al. (2016) Absence of residual structure in the intrinsically disordered
  537 regulatory protein CP12 in its reduced state. Biochem. Biophys. Res. Commun. 477,
  538 20-26
- 37. Robbens, S. *et al.* (2007) Unique regulation of the Calvin cycle in the ultrasmall
  green alga Ostreococcus. J. Mol. Evol. 64(5), 601-604.
- 54138. Petersen, J. (2006) The GapA/B gene duplication marks the origin of Streptophyta542(charophytes and land plants). Mol. Biol. Evol. 23, 1109-1118
- 543 39. Marri, L. *et al.* (2014) CP12-mediated protection of Calvin-Benson cycle enzymes
  544 from oxidative stress. Biochimie 97, 228-237
- 545 40. Marri, L. *et al.* (2008) Spontaneous assembly of photosynthetic supramolecular
  546 complexes as mediated by the intrinsically unstructured protein CP12. J. Biol. Chem.
  547 283, 1831-1838
- 548 41. Fermani, S. *et al.* (2012) Conformational selection and folding-upon-binding of
  549 intrinsically disordered protein CP12 regulate photosynthetic enzymes assembly. J.
  550 Biol. Chem. 287, 21372-21383
- 42. Reichmann, D. and Jakob, U. (2013) The roles of conditional disorder in redox
  proteins. Curr. Opin. Struct. Biol. 23, 436-442

- 43. Launay, H. *et al.* (2018) Cryptic Disorder Out of Disorder: Encounter between
  Conditionally Disordered CP12 and Glyceraldehyde-3-Phosphate Dehydrogenase.
  J. Mol. Biol. 430, 1218-1234.
- 44. Hackenberg, C. *et al.* (2018) Structural and functional insights into the unique CBSCP12 fusion protein family in cyanobacteria. Proc. Natl. Acad. Sci. U.S.A. 115, 71417146
- 45. Marri, L. *et al.* (2005) Reconstitution and properties of the recombinant
  glyceraldehyde-3-phosphate dehydrogenase/CP12/phosphoribulokinase
  supramolecular complex of Arabidopsis. Plant Physiol. 139, 1433-1443
- 46. Matsumura, H. *et al.* (2011) Structure basis for the regulation of glyceraldehyde-3phosphate dehydrogenase activity via the intrinsically disordered protein CP12.
  Structure. 19, 1846-1854
- 565 47. Wedel, N. and Soll, J. (1998) Evolutionary conserved light regulation of Calvin cycle
  566 activity by NADPH-mediated reversible phosphoribulokinase/CP12/
  567 glyceraldehyde-3-phosphate dehydrogenase complex dissociation. Proc. Natl.
  568 Acad. Sci. U.S.A. 95, 9699-9704
- 569 48. Tamoi, M. *et al.* (2005) The Calvin cycle in cyanobacteria is regulated by CP12 via
  570 the NAD(H)/NADP(H) ratio under light/dark conditions. Plant J. 42, 504-513
- 49. Avilan, L. et al. (2012) CP12 residues involved in the formation and regulation of the
  glyceraldehyde-3-phosphate dehydrogenase-CP12-phosphoribulokinase complex
  in Chlamydomonas reinhardtii. Mol. Biosyst. 8, 2994-3002
- 574 50. Martin, W.F. and Cerff, R. (2017) Physiology, phylogeny, early evolution, and 575 GAPDH. Protoplasma. 254, 1823-1834
- 576 51. Lebreton, S. *et al.* (2003) Modulation, via protein-protein interactions, of
  577 glyceraldehyde-3-phosphate dehydrogenase activity through redox
  578 phosphoribulokinase regulation. J. Biol. Chem. 278, 12078-12084
- 579 52. Howard, T.P. et al. (2008) Thioredoxin-mediated reversible dissociation of a stromal
  580 multiprotein complex in response to changes in light availability. Proc. Natl. Acad.
  581 Sci. U.S.A. 105, 4056-4061
- 582 53. Erales, J. *et al.* (2008) Exploring CP12 binding proteins revealed aldolase as a new 583 partner for the phosphoribulokinase/glyceraldehyde 3-phosphate
- 584 dehydrogenase/CP12 complex--purification and kinetic characterization of this
- 585 enzyme from Chlamydomonas reinhardtii. FEBS J. 275(6), 1248-1259.

- 586 54. Carmo-Silva, A.E. *et al.* (2011) Isolation and compositional analysis of a CP12587 associated complex of calvin cycle enzymes from Nicotiana tabacum. Protein
  588 Pept. Lett. 18(6), 618-624.
- 589 55. Pupillo, P. and Giuliani Piccari, G. (1975) The reversible depolymerization of spinach
  590 chloroplast glyceraldehyde-phosphate dehydrogenase. Interaction with
  591 nucleotides and dithiothreitol. Eur. J. Biochem. 51, 475-482
- 592 56. Baalmann, E. *et al.* (1996) Functional studies of chloroplast glyceraldehyde-3-593 phosphate dehydrogenase subunits A and B expressed in *Escherichia coli*: 594 formation of highly active A4 and B4 homotetramers and evidence that 595 aggregation of the B4 complex is mediated by the B subunit carboxy terminus. 596 Plant Mol. Biol. 32, 505-513
- 597 57. Scagliarini, S. *et al.* (1998) The non-regulatory isoform of NAD(P)-glyceraldehyde-3-598 phosphate dehydrogenase from spinach chloroplasts. J. Exp. Bot. 49, 1307-1315.
- 599 58. Sparla, F. et al. (2002) The C-terminal extension of glyceraldehyde-3-phosphate
  600 dehydrogenase subunit B acts as an autoinhibitory domain regulated by
  601 thioredoxins and nicotinamide adenine dinucleotide. J. Biol. Chem. 277, 44946602 44952
- 59. Fermani, S. *et al.* (2007) Molecular mechanism of thioredoxin regulation in
  photosynthetic A2B2-glyceraldehyde-3-phosphate dehydrogenase. Proc. Natl.
  Acad. Sci. U.S.A. 104, 11109-11114
- 606 60. Scheibe, R. *et al.* (2002) Co-existence of two regulatory NADP-glyceraldehyde 3-P
  607 dehydrogenase complexes in higher plant chloroplasts. Eur. J. Biochem. 269, 5617608 5624
- 609 61. Howard, T.P. *et al.* (2011) Inter-species variation in the oligomeric states of the
  610 higher plant Calvin cycle enzymes glyceraldehyde-3-phosphate dehydrogenase
  611 and phosphoribulokinase. J. Exp. Bot. 62,3799-3805

612 62. Scagliarini, S. et al. (1993). Light activation and molecular-mass changes of NAD(P)613 glyceraldehyde 3-phosphate dehydrogenase of spinach and maize leaves. Planta
614 190, 313–319

- 615 63. Nikkanen, L. *et al.* (2016) Crosstalk between chloroplast thioredoxin systems in 616 regulation of photosynthesis. Plant Cell Environ. 39, 1691-1705
- 64. Pérez-Ruiz, J.M. (2017) NTRC-dependent redox balance of 2-Cys peroxiredoxins is
  618 needed for optimal function of the photosynthetic apparatus. Proc. Natl. Acad. Sci.
  619 U.S.A. 114, 12069-12074

- 620 65. Vaseghi, M.J. et al. (2018) The chloroplast 2-cysteine peroxiredoxin functions as
  621 thioredoxin oxidase in redox regulation of chloroplast metabolism. Elife.
  622 DOI:10.7554/eLife.38194 https://elifesciences.org/
- 623 66. Ojeda, V. *et al.* (2018) 2-Cys Peroxiredoxins Participate in the Oxidation of 624 Chloroplast Enzymes in the Dark. Mol. Plant. 11, 1377-1388.
- 625 67. Yoshida, K. et al. (2018) Thioredoxin-like2/2-Cys peroxiredoxin redox cascade
  626 supports oxidative thiol modulation in chloroplasts. Proc. Natl. Acad. Sci. U.S.A. 115,
  627 E8296-E8304.
- 628 68. Yoshida, K. *et al.* (2019) New Light on Chloroplast Redox Regulation: Molecular
  629 Mechanism of Protein Thiol Oxidation. Front. Plant Sci. 10, 1534.

630 DOI:10.3389/fpls.2019.01534 (https://www.frontiersin.org/journals/plant-science)

- 631 69. Howard, T.P. *et al.* (2011) Antisense suppression of the small chloroplast protein CP12
  632 in tobacco alters carbon partitioning and severely restricts growth. Plant Physiol.
  633 157, 620-631
- 634 70. Hammel, A. *et al.* (2020) Overexpression of Sedoheptulose-1,7-Bisphosphatase
  635 Enhances Photosynthesis in *Chlamydomonas reinhardtii* and Has No Effect on the
  636 Abundance of Other Calvin-Benson Cycle Enzymes. Front. Plant Sci.
- 637 DOI:10.3389/fpls.2020.00868 (https://www.frontiersin.org/journals/plant-science)
- 638 71. Heineke, D. *et al.* (1991) Redox Transfer across the Inner Chloroplast Envelope
  639 Membrane. Plant Physiol. 95, 1131-1137
- 64072. Thompson, L.R. et al. (2011) Phage auxiliary metabolic genes and the redirection of641cyanobacterial host carbon metabolism. Proc. Natl. Acad. Sci. U.S.A. 108:E757-E764
- 642 73. Thompson, L.R. *et al.* (2016) Gene Expression Patterns during Light and Dark
  643 Infection of Prochlorococcus by Cyanophage. PLoS One,

644 DOI:10.1371/journal.pone.0165375 (https://journals.plos.org/plosone)

- 645 74. Kanno, M. et al. (2017) Global metabolic rewiring for improved CO2 fixation and
  646 chemical production in cyanobacteria. Nat. Commun. DOI:10.1038/ncomms14724
  647 (https://www.nature.com/articles/ncomms)
- 648 75. Marri, L. *et al.* (2005) Co-ordinated gene expression of photosynthetic
  649 glyceraldehyde-3-phosphate dehydrogenase, phosphoribulokinase, and CP12 in
  650 Arabidopsis thaliana. J. Exp. Bot. 56, 73-80
- 651 76. Singh, P. *et al.* (2008) Expression analysis of the Arabidopsis CP12 gene family
  652 suggests novel roles for these proteins in roots and floral tissues. J. Exp. Bot. 59, 3975653 3985

- 654 77. López-Calcagno E.P. *et al.* (2017) Arabidopsis CP12 mutants have reduced levels of
  655 phosphoribulokinase and impaired function of the Calvin-Benson cycle. J Exp Bot.
  656 68, 2285-2298
- 657 78. Lin, Q. et al. (2020) Prime genome editing in rice and wheat. Nat Biotechnol. 38,
  658 582-585
- 659 79. Michelet, L. *et al.* (2013) Redox regulation of the Calvin-Benson cycle: something
  660 old, something new. Front. Plant Sci. DOI:10.3389/fpls.2013.00470
- 661 80. Figge, R.M. *et al.* (1999) Glyceraldehyde-3-phosphate dehydrogenase gene
  662 diversity in eubacteria and eukaryotes: evidence for intra- and inter-kingdom gene
  663 transfer. Mol. Biol. Evol. 16, 429-440
- 664 81. Petersen, J. *et al.* (2003) Origin, evolution, and metabolic role of a novel glycolytic 665 GAPDH enzyme recruited by land plant plastids. *J. Mol. Evol.* 57, 16-26
- 666 82. Rae 2010
- 667

# 668 **OUTSTANDING QUESTIONS**

- Which is the dynamics of diphosphorylated (NAD) versus triphosphorylated (NADP)
   pyridine nucleotides in higher plants chloroplasts in light/dark cycles and fluctuating
   light conditions?
- Are dark-complexes (GAPDH/CP12/PRK and A<sub>8</sub>B<sub>8</sub>-GAPDH) of land plants important
   for adaptation to fluctuating light?
- Is NTRC (NADPH-thioredoxin C) important for dark-complexes dissociation?
- Is the recently described electron chain based on atypical thioredoxins ACHT/TRXL 2 and 2-cys peroxiredoxins important for dark-complexes association?
- How the CP12-derived C-terminal extension of subunits B makes A<sub>2</sub>B<sub>2</sub>-GAPDH of
   land plants able to auto-assemble in A<sub>8</sub>B<sub>8</sub>-GAPDH and other types of GAPDH complexes? Complexes of AB-GAPDH are the only elements of the regulatory
   system of GAPDH and PRK in land plants whose tridimensional structure is not yet
   know.
- How the dynamics of dark-complexes formation and dissociation could be
   detected *in vivo* in real time?
- How do complexes relate to stress conditions in vivo? Reactive oxygen species are
   produced in several types of stress and, in vitro, hydrogen peroxide oxidizes CP12
   and induces aggregation/protection of GAPDH and PRK, but whether this
   mechanism is relevant in vivo is not yet known.

- Can the effect of CP12 in protecting PRK from proteolysis in Arabidopsis thaliana be
   extended to other species and/or other types of complexes like A<sub>8</sub>B<sub>8</sub>-GAPDH?
   Whether dark-complexes may have a general role in proteostasis is not yet known.
- Why land plants have so many regulatory mechanisms of the Calvin-Benson cycle
   at the level of GAPDH and PRK, with apparently overlapping functions? AB-GAPDH
   and PRK are both redox-regulated, both individually and through CP12; AB-GAPDH
   and A<sub>4</sub>-GAPDH/PRK are both able to form inactive complexes under similar control
   (thioredoxins and pyridine nucleotides).
- 696

### 697 **LEGENDS TO FIGURES**

698 Figure 1. Photosynthesis is a redox-regulated redox process. (a) The oxidation state of C in 699  $CO_2$  is (+4). The average oxidation state of C atoms in sugars is (0). Rubisco adds a  $CO_2$  (+4) 700 to RuBP (0) generating two molecules of PGA (+2 x 2). PGK adds ATP to PGA, and GAPDH 701 uses four electrons (e-) from NADPH to reduce BPGA (+2 x 2) to G3P (0). NADPH is derived 702 from light reactions of photosynthesis. The electron transport is coupled to trans-thylakoidal 703 proton motive force that generates ATP via ATP-synthase. G3P regenerates Ru5P in a series 704 of reactions with P-sugar intermediates (not shown). Two irreversible phosphatases drive the 705 Ru5P regeneration from G3P. PRK and PGK restore the phosphates lost by the cycle. (b) In 706 oxygenic phototrophs, PRK and GAPDH can form a regulatory complex with CP12. The 707 hierarchical process of aggregation is structurally characterized. GAPDH [27,28] forms a 708 binary complex with CP12 when NAD(H) substitutes NADP(H) in GAPDH and CP12 is oxidized 709 (4 electrons) and bears two disulfides [52,58]. PRK is redox-regulated [14,16,17] and both PRK 710 forms can bind the GAPDH/CP12 binary complex to form the ternary complex 711 GAPDH<sub>2</sub>/CP12<sub>4</sub>/PRK<sub>2</sub> in which both enzymes are strongly inhibited [17,19]. Complex dissociation and enzyme reactivation is obtained by reduced thioredoxins or NADP(H) or 712 713 BPGA or ATP, with different efficiency [79]. Abbreviations: BPGA, 1,3-bisphosphoglyceric 714 acids; CET, cyclic electron transport; G3P, glyceraldehyde-3-phosphate; GAPDH, 715 glyceraldehyde-3-phosphate dehydrogenase; LET, linear electron transport; OEC, oxygen 716 evolving complex; PGA, 3-phosphoglyceric acid; PGK, phosphoglycerate kinase; PQ, 717 plastoquinone; PRK, phosphoribulokinase; PSI, photosystem I; PSII, photosystem II; Ru5P, 718 ribulose-5-phosphate; RuBP, ribulose-1,5-bisphosphate; TRX, thioredoxin.

719

Figure 2. Phosphoribulokinase: structure and regulation. (a) Dimer of algal PRK
 (Chlamydomonas reinhardtii, [16]), the left subunit is represented as surface potential (red,

722 negative; blue, positive), the right subunit as cartoon with cysteines as yellow spheres. The 723 large positive area between C16 and C55 corresponds to the active site. The C16-C55 724 disulfide inhibits PRK activity. The C243-C249 disulfide has no effects on activity but is 725 commonly found in ternary complexes. The lid (green) is suspected to move during catalysis. 726 Correspondence between A. thaliana and C. reinhardtii Cys numbering is shown on top of 727 the panel. (b) Algal PRK overview with the central 18-strands  $\beta$ -sheet highlighted in colours. 728 The small dimer interface is represented by two short  $\beta$ -strands (red). (c) Cyanobacterial PRK 729 active site with substrate analogues (Synechococcus elongatus, [17]). G6P and ADP are 730 located in Ru5P and ATP sites, respectively. The positive surface of the binding sites is 731 complementary to the negative phosphate groups. Histidine-106 (H106) and aspartate-58 732 (D58) form the catalytic base activating carbon-1 of Ru5P. (d) Reduce/active (blue) and 733 oxidized/inactive (red) plant PRK (Arabidopsis thaliana, [17]). The movement of the P-loop 734 represents the only relevant structural difference between reduced and oxidized PRK. After 735 P-loop flipping, C15 and C54 are close enough to form a disulfide that distorts the active 736 site and inhibits PRK activity. (e) CP12 (yellow cartoon) inhibits PRK (surface potential) 737 occupying its active site (detail from the arabidopsis GAPDH<sub>2</sub>-CP12<sub>4</sub>-PRK<sub>2</sub> complex [17], 738 after digital removal of GAPDH). The CP12 consensus sequence (AWD\_VEEL, red) interacts 739 with positive patches of the Ru5P binding site. The approximate positions of the binding sites 740 of ATP and Ru5P are indicated. The lid is open and CP12 prevents it to close. Abbreviations: 741 G6P, glucose-6-phosphate; Ru5P, ribulose-5-phosphate.

742

743 Figure 3. Crystal structures of GAPDH isoforms and A<sub>4</sub>-GAPDH/CP12 binary complex. (a) 744 Typical GAPDH tetramer with subunits in different colours (crystal structure of GAPDH from 745 Spinacia oleracia [30]). In the upper-left subunit, the cofactor-binding domain (salmon) that 746 can bind either NAD(H) or NADP(H) is differentiated from the catalytic domain (red) that 747 binds the substrate. Upper magnification: the 2'-hydroxyl group of NAD(H) (yellow) is 748 stabilized by D32 (yellow), while the 2'-phosphate of NADP(H) (cyan) interacts with R77 and 749 T33 (cyan), and \$188 of the S-loop of the adjacent subunit (light-blue). In bispecific GAPDHs 750 the binding of NADP(H) is made possible by the rotation of D32 (cyan) away from the 2'-751 phosphate of NADP(H). Dashed lines indicate interactions  $\leq$  4 Å [28,30]. Lower 752 magnification: the active site contains the C149-H176 catalytic pair. The Pi and Ps sites 753 allocate BPGA phosphate groups (substituted by sulphate ions in the crystal structure) [30]. 754 (b) In the A<sub>4</sub>-GAPDH/CP12 binary complex, the C-terminus of CP12 (cyan) fits into the cleft 755 separating two A-GAPDH subunits, with Y76 and N78 occupying the P-sites of the light-blue 756 subunit, preventing substrate binding, while E72 prevents NADP(H)-binding to the opposite

757 (yellow) subunit [41]. (c) In A<sub>2</sub>B<sub>2</sub>-GAPDH, oxidized CTE (green) occupies the cleft between B 758 (light-green) and A (sand) subunits, similarly to CP12 in the binary complex. However, CTE 759 does not occupy the P-sites but causes the 2'-phosphate of NADP(H) of the B-subunit (light-760 green) to loose crucial interactions with T33, R77 and S188, which are responsible for the 761 high NADP(H)-dependent activity of the enzyme [59]. Atom colour codes: oxygen red; 762 nitrogen blue; sulphur yellow.

763

764 Figure 4. Current view of GAPDH/PRK regulation based on combined in vivo and in vitro 765 evidence. The model is based on data collected from different organisms and its general 766 principles apply to cyanobacteria, green algae and land plants, although AB-GAPDHs are 767 only found in land plants [58]. From left to right: at variable light conditions, redox-sensitive 768 proteins CP12, PRK and A<sub>2</sub>B<sub>2</sub>-GAPDH equilibrate with thioredoxins and tend to be reduced, enzymatically active and free from complexes [79]. In light-to-dark transitions, atypical 769 770 thioredoxins (ACHT, TRXL-2) with less negative redox potential than thioredoxins f and m [68], 771 convey electrons from reduced targets to hydrogen peroxide via 2-cys peroxiredoxins [66-772 69]. Chloroplast NADP(H)/NAD(H) ratio tend to decrease in the dark [4,72], favouring the 773 substitution of NADP(H) with NAD(H) in bispecific GAPDHs. Oxidation of CP12 and C-terminal 774 extension (CTE) of GAPDH B-subunits, and low NADP(H)/NAD(H) ratios, favour the formation 775 of dark-complexes of inactive enzymes (GAPDH<sub>2</sub>CP12<sub>4</sub>PRK<sub>2</sub> and A<sub>8</sub>B<sub>8</sub>-GAPDH)[17,19,48,55]. 776 In dark-to-light transitions and then in full light, dark complexes are dissociated and enzyme 777 activities fully recovered. Thioredoxins f and m, reduced by ferredoxin-thioredoxin 778 reductase at the onset of light reduce CP12 and CTE disulfides, causing dark-complexes 779 dissociation [24,55]. NADPH-thioredoxin C (NTRC) may contribute to the same effect [64,65]. 780 Complexes dissociation is aided by NADPH, BPGA and ATP, all able to bind in different 781 positions and cause CP12 or CTE displacement from their binding sites [45,48,59]. Dashed 782 arrows indicate interactions that are not fully proven yet. Abbreviations: 2CP, 2-cys-783 peroxyredoxins; BPGA, 1,3-bisphosphoglyceric acids; CTE; C-terminal extension of GAPDH 784 B-subunits; GAPDH, glyceraldehyde-3-phosphate dehydrogenase; NTRC, NADPH-785 thioredoxin C; PRK, phosphoribulokinase; TRX, thioredoxin.

- 786
- 787 **TEXT BOXES**
- 788

#### 789 Box 1 - Evolution and biodiversity of GAPDH, PRK and CP12 along the green lineage 790

- 791 Early times: before primary endosymbiosis

792 Early eukaryotes contained a NAD-specific GAPDH isoform of eubacterial origin, localized 793 in the cytosol and involved in glycolysis. This prototypical GAPDH, named C<sub>4</sub>-GAPDH and 794 coded by GAPC genes, is ubiquitously expressed in present eukaryotes [51] (Figure I). 795 Cyanobacteria, early and present ones, contain a C4-like GAPDH, coded by GAP1 genes, 796 but also a GAPDH of the A<sub>4</sub>-type coded by GAP2 genes [80]. A<sub>4</sub>-GAPDH is characterized by 797 the double specificity for pyridine nucleotides and the role in the Calvin-Benson cycle. Early 798 cyanobacteria, also contained PRK and canonical CP12 with conserved N- and C-terminal 799 disulfides and central consensus sequence [73], hence potentially able to bind A4-GAPDH 800 and PRK [10].

- 801
- 802

#### 803 Origin of photosynthetic eukaryotes

804 Early photosynthetic eukaryotes formed by primary endosymbiosis contained C<sub>4</sub>-GAPDH 805 derived from the eukaryotic host and A4-GAPDH of cyanobacterial origin located in 806 chloroplasts, together with PRK and canonical CP12. GAP1 genes coding for 807 cyanobacterial C4-GAPDH were apparently lost after endosymbiosis. The set of genes coding for GAPDH (GAPC and GAPA), CP12 and PRK in early photosynthetic eukaryotes is 808 809 typically found conserved in green algae and land plants of present days, possibly with 810 paralogues derived from whole genome duplications [10,73,51]. Unicellular 811 prasinophycean algae (an early diverging group of green algae with members that are 812 prominent in the oceanic picoplankton) like Ostreococcus tauri represent an exception in 813 having no CP12 in their genome[37].

814

#### 815 CP12 and PRK biodiversity in cyanobacteria

816 Besides canonical CP12 genes, cyanobacteria may also contain genes for CP12 variants 817 that are not found in green photosynthetic eukaryotes [73]. These include CP12 isoforms 818 with no C-terminal cysteines and/or N-terminal cysteines and/or central consensus 819 sequence. Oceanic species included in genera Prochlorococcus and Synechococcus and 820 belonging to the phylogenetic a-group of cyanobacteria (Rae 2010)[82] are an exception 821 in having no canonical CP12 genes but only variants without consensus sequence and thus 822 unable to bind PRK [73]. Oceanic a-cyanobacteria are an exception also for PRK, that is a 823 bacterial-type (octameric) [18]. Several species of cyanobacteria outside a-cyanobacteria 824 may also contain, besides canonical CP12, cystathionine beta-synthase (CBS)-CP12 fusion 825 proteins in which two CBS domains are fused to a canonical CP12 and form hexamers that

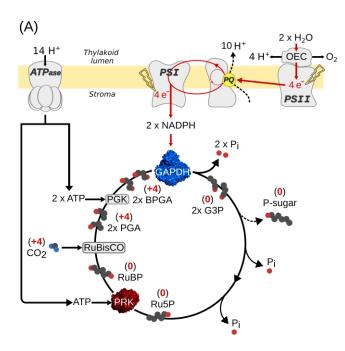
bind/inhibit PRK in an AMP-dependent manner, thereby potentially interfering with PRKredox activation [44].

- 828
- 829 Land plants

830 At the origin of land plants evolution another GAPDH isoform (A<sub>2</sub>B<sub>2</sub>-GAPDH) appeared as a 831 result of a gene fusion between a duplicated GAPA gene and the C-terminal domain of CP12 [58] that gave rise to GAPB genes. A<sub>2</sub>B<sub>2</sub>-GAPDH shows CP12-derived regulatory 832 833 properties. Green algae Ostreococcus tauri and related species, are the only known 834 examples of organisms outside Streptophyta (land plants and charophytes) to have both 835 GAPA and GAPB genes, the latter possibly recruited by horizontal gene transfer [37]. Land plants also contain Cp<sub>4</sub>-GAPDH in plastids, particularly heterotrophic ones, derived from 836 837 GAPC [81]. Land plants thus contain four GAPDH isoforms (cytosolic C<sub>4</sub>; chloroplastic A<sub>4</sub> and 838 A<sub>2</sub>B<sub>2</sub>; plastidial Cp<sub>4</sub>), together with PRK and canonical CP12, able to build complexes with 839 PRK and GAPDH ( $A_4$  or  $A_2B_2$ ) but not with Cp4-GAPDH [9]. 840

Figure I – Schematic representation of the evolution and biodiversity of GAPDH, PRK and
CP12 along the green lineage and in cyanobacteria

- 843
- 844
- 845



(B)

